

TRANSPORTATION OF NANOCELLULOSE DISPERSIONS THROUGH POROUS MEDIA

Reidun Cecilie Aadland⁽¹⁾, Carter Jordan Dziuba⁽²⁾, Ellinor Bævre Heggset⁽³⁾, Kristin Syverud^(1,3), Ole Torsæter^(1,4), Ian D. Gates⁽²⁾ and Steven Bryant⁽²⁾

- 1) Norwegian University of Science and Technology (NTNU), Trondheim, Norway
- 2) Department of Chemical and Petroleum Engineering, University of Calgary, 2500 University Dr. N.W., Calgary, Alberta T2K-1N4
- 3) RISE PFI, Trondheim, Norway
- 4) PoreLab, Department of Geoscience and Petroleum, NTNU, 7491 Trondheim, Norway

This paper was prepared for presentation at the International Symposium of the Society of Core Analysts held in Vienna, Austria, 27 August – 1 September 2017

ABSTRACT

Nanocellulose serves as a potential new water additive for enhanced oil recovery (EOR) applications. This is an emerging new type of nanoparticle that is comprised of cellulose fibrils in the nanometer range. Cellulose is a biopolymer and it is the main constituent in the cell wall of plants and trees. Thus, the material is biodegradable, non-toxic and renewable. The particles are different from traditional nanoparticles, such as silica, since they are rod-shaped instead of spherical. This adds a new element of complexity to their flow behavior.

Transportation of nanocellulose through porous media has been investigated where the main objective was to identify retention mechanisms. Experiments consisted of single-phase flow through unconsolidated sandpacks. Two floods were performed for each experiment – a tracerflood and a nanoflood. An ultraviolet (UV)-visible (VIS) spectrometer was used to measure the nanocellulose concentration, and pressure data gave information about permeability alterations. The effects of varying the salinity, sand grain size, particle size and velocity were examined. Two types of cellulose nanocrystals (CNC) were tested: CNC from the U.S. Department of Agriculture (USDA) and CNC from Alberta Innovates Technology Futures (AITF).

From these experiments, it is clear that nanocellulose particles, suspended in aqueous phase, have the ability to flow through porous media. As a general trend, it was observed that larger particles or aggregates resulted in higher retention and permeability impairment. By increasing the salinity, particles started to aggregate more, which resulted in blocking and log-jamming in the sandpack. Thus, salinity was found to be the most important parameter affecting transport. For larger particles, the main retention mechanism was observed to be log-jamming, whereas for small particles adsorption was observed.

Furthermore, higher velocities or larger grain sizes were found to reduce retention and permeability reduction.

INTRODUCTION

Over the last decades, production rates from existing fields have declined since most of the easy and accessible oil has already been produced. The remaining oil is difficult to extract and there is a low proportion of new fields for exploration. As a result, there is a constant need for environmental friendly EOR methods that are more efficient and less expensive than the ones we have today. Chemical flooding with polymers is considered one of the most promising EOR methods and has been researched for over 40 years¹.

The aim of the method is to mix the polymer with water to enhance the viscosity of the injection fluid. By injecting a more viscous fluid, the mobility ratio will become favourable and the macroscopic sweep efficiency will be improved. The viscosity can be enhanced by increasing the size of the polymer (i.e. the molecular weight). However, a larger size increases the risk of plugging of pore throats and formation damage. Polymers are also easily adsorbed onto solid surfaces, which results in loss of chemicals to the formation. Loss of chemicals will in turn increase the injection cost, as it is necessary to inject more polymers to maintain the desired concentration. Thus, the method faces challenges². To increase EOR efficiency of injection fluids, particles should therefore be small enough to allow for long distance transport in the subsurface with minimal retention.

The research reported in this paper focuses on a novel green nanoparticle, nanocellulose, for chemical EOR applications. Nanocellulose is comprised of cellulose fibrils in the nanometer range, hence they are much smaller than polymers. Cellulose is a biopolymer obtained from wood (Fig.1), thus it is a renewable resource with relatively low toxicity. Nanoscale cellulose particles may be classified into three main subcategories: bacterial nanocellulose (BNC), cellulose nanofibers (CNF) and cellulose nanocrystals (CNC)³. Only the latter category has been studied in this paper.

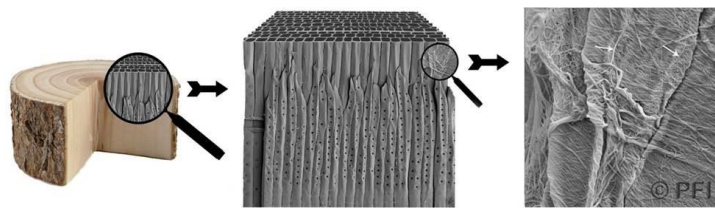


Figure 1. From tree to nanocellulose. Photo by Per Olav Johnsen, RISE PFI

Nanocellulose is an emerging new type of nanoparticle in the petroleum industry. Hence, there does not exist a lot of research on its applications for EOR. Molnes et al. (2016)⁴ looked into the premise for use of CNC in EOR. Through their research, it was established that stable dispersions of CNC were obtained when using 1000 ppm NaCl brines as a dispersing medium. In their study cellulose nanocrystal concentrations ranging from 0.5 to 2.0 wt.% were tested. All dispersions remained stable and the stability was verified through zeta-potential measurements. Furthermore, the CNC dispersion was injectable through a

sandstone core. Nevertheless, there were indications that some of the CNC particles became trapped inside the pore matrix, which is a common phenomenon when dealing with polymers⁴.

When nanoparticles flow through porous media, there are four potential transport outcomes - adsorption, blocking, bridging (log-jam) or free passage (Fig. 2). The first scenario might occur if the nanoparticle is much smaller than the pore size and there exist some physiochemical interaction between the particle and the pore wall. The particles will then adsorb to the pore wall, which could lead to a wettability change. This adsorption can be reversible or irreversible. Blocking could take place if the particle is much larger than the pore throat. Bridging or log jamming of the pore throat arises when two or more particles with sizes slightly less than a pore throat accumulate together, leading to an obstruction of the pore throat. Free passage happens if the pore throat is large, in which nanoparticles can easily move through⁵.

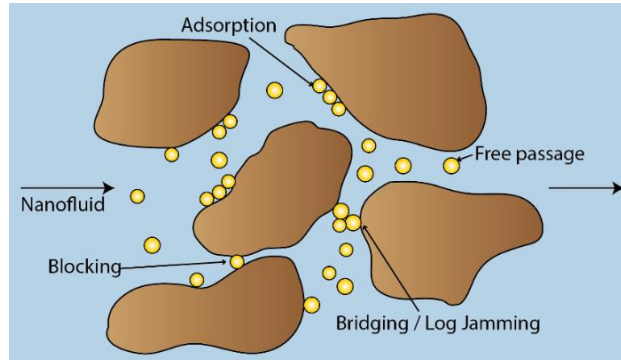


Figure 2. Possible transport outcomes for nanoparticles flowing through porous media.

The aim of this study was to identify the main retention mechanism that affects transport of nanocellulose through porous media. Nanocellulose particles are not spherical, but rod-shaped, which adds complexity to potential flow behavior.

MATERIALS

Porous media

The porous media consisted of a 1-ft-long column (inner diameter = 0.62 inches), which was packed with silica sand grains. The sand grains were purchased from Sigma-Aldrich and Agsco. In the experiments, three different grain sizes were used: large (16-30 mesh), medium (50-70 mesh) and small (140-270 mesh). For the majority of the experiments the medium grain size was used. The average physical properties are listed in Table 1.

Table 1. Average properties of the sandpacks used in retention flooding experiments

Sand Grain Size		Porosity	Permeability	Pore Volume
[mesh]	[μm]	[%]	[D]	[ml]
140-270	53-105	39	3	23.6
50-70	210-297	37	35	22.1
16-30	595-1190	33	284	19.6

Brine

In the majority of the retention experiments 0.1 wt.% brine was used, which was prepared using sodium chloride (NaCl). To test the effect of salinity on nanocellulose transport, experiments were also conducted using 0.3 wt.% and 1.0 wt.% brine.

Nanocellulose

Two types of cellulose nanocrystals (CNC) were used in this study. One was purchased from the University of Maine. This material was manufactured at the Forest Products Laboratory in Madison, USDA (U.S. Dep. of Agriculture). The cellulose nanocrystals were produced using 64 % sulphuric acid to hydrolyze the amorphous regions of the cellulose material, resulting in acid resistant crystals⁶. The stock dispersion is in a gel-form and has a concentration of 12 wt.%. This CNC is denoted CNC (USDA) in this article. The other type of CNC was purchased from Alberta Innovates Technology Futures, and is denoted CNC (AITF). These cellulose nanocrystals were also prepared by using concentrated sulphuric acid. The production process for CNC (AITF) has a spray-drying step so the final nanocellulose product is in powder form instead of gel form.

Both nanocellulose types were diluted to 0.5 wt.% with the respective brine – 0.1 wt.%, 0.3 wt.% or 1.0 wt.% NaCl.

EXPERIMENTAL METHODS

Particle size and zeta potential

The size of nanocellulose aggregates was measured by using dynamic light scattering (DLS). For each solution, 25 sizing measurements were taken and any measurements with an intensity more than one standard deviation from the median intensity were omitted. The remaining measurements were averaged. Zeta potential measurements were taken as the average of six measurements. All dynamic light scattering measurements and zeta potential measurements were performed with a NanoPlus HD zeta/nano particle analyzer.

Flooding setup

Figure 3 shows a schematic of the flooding setup. All experiments were conducted at ambient conditions. A syringe pump was used to inject either nanocellulose fluid or brine through the horizontal sandpack. An in-line ultraviolet (UV)-visible (VIS) spectrometer gave the absorbance readings of the fluid, which was used to calculate a mass balance around the sandpack. The pressure drop across the sandpack was measured throughout the experiment, which gave information about permeability alterations.

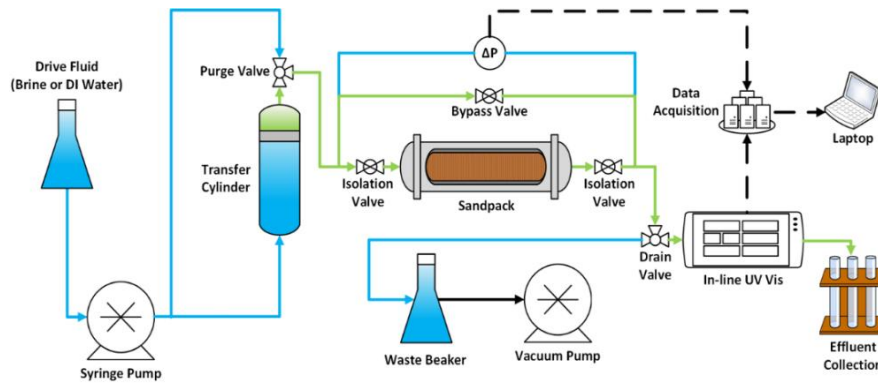


Figure 3. Schematic of the experimental setup used for retention floods

Experimental procedure

One flooding experiment took approximately two days to complete; where day one was injection of a tracer fluid and day two was injection of the nanofluid (NF). There were two main procedures for each experiment: a preparation part and the tracerflood or nanoflood. Four different parameters were varied in these floods: salinity, grain size, particle type and velocity (Table 2).

Table 2. Details over the conducted retention floods. The tables (A-D) list the parameters and values that were tested for each flood. The initial concentration of CNC was 0.5 wt.% for all experiments.

A. Particle type				C. Grain size			
Particle type	Sand grain size [mesh]	Salinity [wt.%]	Darcy velocity [cm/min]	Particle type	Sand grain size [mesh]	Salinity [wt.%]	Darcy velocity [cm/min]
CNC (USDA)	50-70	0.1	0.5	CNC (USDA)	140-270	0.1	0.5
CNC (AITF)	50-70	0.1	0.5	CNC (USDA)	50-70	0.1	0.5
				CNC (USDA)	16-30	0.1	0.5
B. Velocity				D. Salinity			
Particle type	Sand grain size [mesh]	Salinity [wt.%]	Darcy velocity [cm/min]	Particle type	Sand grain size [mesh]	Salinity [wt.%]	Darcy velocity [cm/min]
CNC (AITF)	50-70	0.1	0.05	CNC (USDA)	50-70	0.1	0.5
CNC (AITF)	50-70	0.1	0.5	CNC (USDA)	50-70	0.3	0.5
CNC (AITF)	50-70	0.1	4.1	CNC (USDA)	50-70	1.0	0.5

Preparation of sandpacks

The sand was rinsed over a sieve using deionized water (DIW) and high salinity brine (10 wt. % NaCl). It was then dried in an oven before packing. After packing the tube with sand,

a vacuum pump was used to remove all the water from the lines in the system. The sandpack was afterwards saturated with DIW. The sandpack was prepared for the tracerflood or nanoflood by alternating between injection of DIW at a high rate (29 ml/min) and 10 wt.% brine at a low rate (2 ml/min). This preparation step was done to knock out silica fines that might disturb the UV-Vis absorbance readings during the actual floods. The final step of the preparation part was to purge the sandpack with the salinity that was going to be used in the NF. This purge continued until the UV-Vis signal leveled out.

Sandpack flooding procedure

Sodium Iodide (NaI) was used as the tracer, and the tracerflood was carried out with each sandpack before nanocellulose injection. The tracerflood was injected to characterize the dispersivity in the sandpacks. After each experiment the tracer breakthrough (BT) curve was compared to the nanocellulose BT-curve. Normally, two pore volumes (PV) of tracer was injected, followed by three PV of brine post flush. Afterwards, the sandpack was prepared for the nanocellulose injection by again alternating between DIW and high salinity brine, as described above. The nanocellulose injection followed the same procedure as the tracerflood, with two PV of nanocellulose injection and then three PV of post flush.

Visualizing nanocellulose retention

Nanocellulose shows significant thermal decomposition at high temperatures. Heggset et. al (2017) evaluated the temperature stability of nanocellulose dispersions and found that nanocellulose start to degrade around 110°C⁷. The thermal decomposition results in production of black ash and some char. After each flood, the sand from the pack was emptied onto a tinfoil sheet by applying low-pressured air to the outlet side of the pack, pushing the sand slowly out. It was then baked in a Thermo Scientific HERATHERM Oven at 300°C to trigger thermal decomposition. Regions of the sandpack containing relatively more nanocellulose would darken more than the rest of the pack due to the presence of ash and char. This allowed for a qualitative visualization of the retention.

RESULTS AND DISCUSSION

Particle size and zeta potential

Table 3 shows the average measured particle size values and the zeta potential for the solutions that were used in the retention flooding experiments. The size of the particles in deionized water (DIW) is also included in the table as a reference for the onset of aggregation. Dynamic light scattering is a technique which is intended for spherical particles, so the measurements in this section is not an exact value of their size, but gives the possibility to compare the samples to one another.

Table 3. Aggregate sizing data (measured by DLS) and zeta potential data for the fluids used in the floods. The zero salinity value corresponds to the nominal particle size.

	0.5 wt.% CNC (USDA)				0.5 wt.% CNC (AITF)	
	0	0.1	0.3	1	0	0.1
Salinity [wt.%]						
Avg. Aggregate size [nm]	53 ±3	67 ±3	298 ±12	913 ±132	166 ±15	321 ±29
Zeta potential [mv]	-	-30.28 ±1.18	-21.20 ±2.37	-11.01 ±1.32	-	-23.60 ±2.22

Retention flooding results

This section presents a series of selected BT-curves outlining the key findings from the flooding experiments (Fig. 4-6). When reading the BT-curves, note that the black dotted curve is the tracer. The tracer curve was run prior to each experiment, and by comparing all of them against each other the curves overlays with minimal variation to the top-, start- or ending-point. The curve is intended to map the dispersion of the sandpack for an ideal case of no retention. The nanocellulose BT-curves are compared against the tracer curve to identify various transport phenomena occurring during the floods. The graphs also contain the corresponding pressure curves for each experiment. This data gives information about permeability impairment in the sandpack. The results for each tested parameter (particle type, velocity, grain size and salinity) are presented below. The retention and permeability data from the floods is found in Table 4.

1. Impact of particle type

The two tested particle types showed different transport behavior in the porous media when tested with the same salinity (0.1 wt.% NaCl). This difference is theorized to be a result of their size. From the DLS measurements, CNC (AITF) aggregates are presumed to be ~4.8 times larger than CNC (USDA) aggregates in 0.1 wt.% NaCl. The flooding experiments showed that the amount of retained particles was in the same range for both types, 6.2 % for CNC (USDA) and 6.6 % for CNC (AITF). The interesting findings were in the permeability data and study of the nanofluid BT-curve. From Figure 4 it is seen that the nanofluid (NF) CNC (USDA) BT-curve is delayed compared to the tracer curve. It is also seen that the pressure curve increases until it reaches one PV. A pressure increase is expected during the first PV as a slightly more viscous fluid is injected into the sandpack. The pressure is then stable for the second PV. Both these observations suggests that some adsorption is taking place. The CNC (USDA) BT-curve has a smooth tail, which suggests that particles are able to transport out of the porous media with minimal straining occurring.

The CNC (AITF) BT-curve on the other hand, overlays with the tracer curve indicating no adsorption is happening. For this flood, other mechanisms seem to be at play. By comparing the pressure curves for the two particles, CNC (AITF) has approximately one and a half times higher pressure than CNC (USDA) during the two PV of nanocellulose injection. This indicates that particles are blocking of pore throats to a greater degree. This log jamming effect is further supported by the continuous increase in pressure during the second PV, and that the brine from the post flush breaks through earlier than the tracer BT-curve. This suggests that pore throats have been blocked off during the nanocellulose flood,

which gives the post flush a smaller volume to traverse before exiting the pack. At the end of the CNC (AITF) tail there is a small bump, which is believed to be retained particles being released from log jams that have been broken apart during the post flush with brine.

Overall, larger nanocellulose particles and aggregates in the bulk solution result in impaired transport properties through porous media.

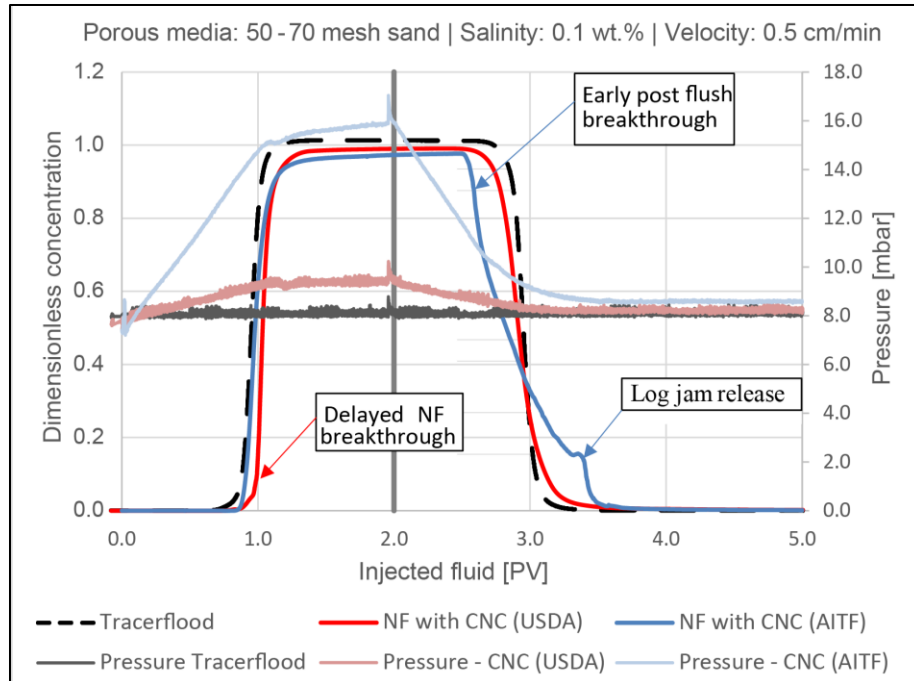


Figure 4. Breakthrough curve for flood with 0.5 wt.% CNC(USDA) (red line) and 0.5 wt.% CNC (AITF) (blue line). The tracer BT-curve is the black dotted line.

2. Impact of velocity

Three velocities were tested in this experiment: a low (0.05 cm/min), medium (0.5 cm/min) and high (4 cm/min). It is believed that a high velocity will result in a high shear rate, which may break up aggregate log-jams. Since CNC (AITF) caused the highest permeability reduction and appeared to be more susceptible to log jamming, they were the only particles considered for the velocity experiments.

The BT and pressure curves for the flooding experiment using the low velocity is seen in Figure 5. The medium velocity was the CNC (AITF) flood that was previously presented in Figure 4. By comparing the floods it is seen that the flood with the low velocity has a much steeper increase in pressure during the second PV of NF injection. The post flush also has an earlier breakthrough compared to the medium velocity, and both floods have some small bumps in the end of the tail for the BT-curve. It is therefore believed that the low velocity leads to more aggregated log jams based on the interpretation of the pressure data and tail of NF curve. From the computed numbers the retention is 24% for the low velocity and 6.6 % for the medium velocity. The overall permeability reduction with the

low velocity is 90.3%. From Figure 5 it is also seen that the pressure drop is spiky and keeps increasing during the post flush. These spikes likely indicate reordering of the retained nanocellulose aggregates. The BT-curves for the high velocity is not included as it behaved almost like a tracer with no early breakthrough of the post flush brine.

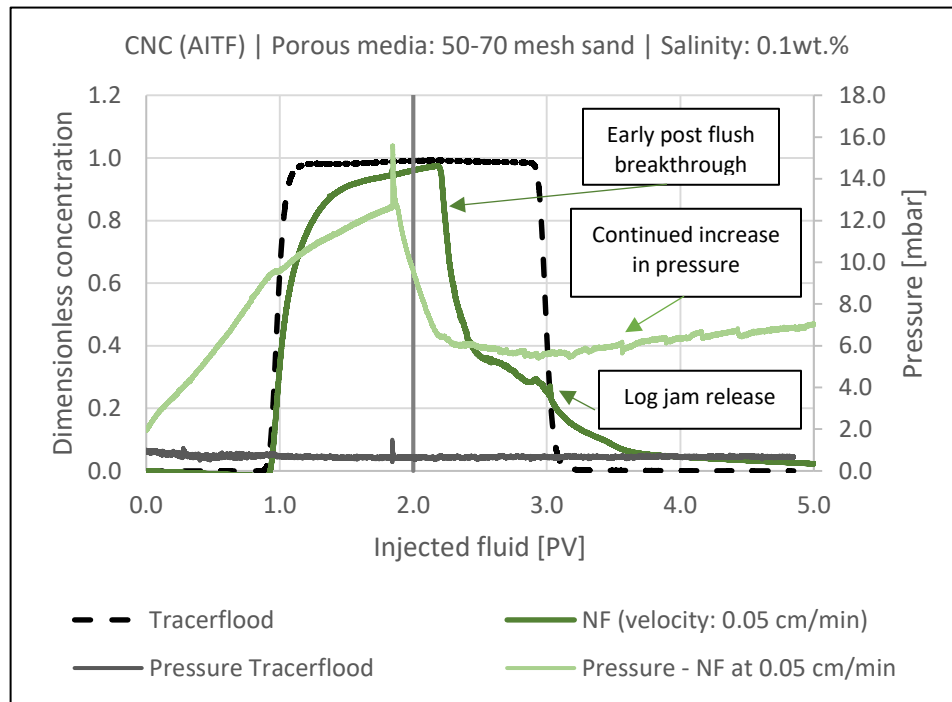


Figure 5. Breakthrough curve for flood with 0.5 wt.% CNC(AITF) (dark green line) using a low velocity (0.05 cm/min). The tracer BT-curve is the black dotted line. The light green and grey line are the corresponding pressure curves.

3. Impact of sand grain size

Only CNC (USDA) was tested with varying the grain size of the sandpack. The major finding from these experiments was that retention and permeability reduction increased as grain size decreased (Table 4). One interesting observation was that the BT-curve for the nanoflood in the medium sand (50-70 mesh) and the small sand (140-270 mesh) were both delayed relative to the tracer curve. The pressure also stabilized during injection of the second PV indicating that no major straining is occurring inside the sandpack. Both these factors suggest that adsorption is occurring, and the effect was slightly more profound for the small sand. The nanoflood BT-curve in the larger sand coincides closely with the tracer curve and there were only 2.3% retention and 3.33% permeability reduction. This implies that this flood was behaving almost like a tracer. No BT-curves are included from these experiments, as they show similar trends as the CNC (USDA) curve in Figure 4.

The grain size will determine how closely packed the sand is, i.e. the diameter in the pores. If the diameter becomes too large, the particles will move relatively unhindered through the porous media with no interaction. In smaller grain sizes, the surface-to-volume ratio is

larger. The results from these three experiments tells us that there seem to be a critical surface area threshold where adsorption starts to come into effect.

4. Impact of salinity

By increasing salinity, the aggregated particle size increases. Thus, this parameter had the most effect on retention and permeability reduction, since larger particles would more easily clog the system. CNC (USDA) was the only particle tested for the effect of salinity, since CNC (AITF) aggregated greatly at salinities above 0.1 wt.%. It was therefore not possible to get a mass balance, as a stable UV reading could not be achieved. Figure 6 show the BT-curve for CNC (USDA) in 0.1 wt.% and 0.3 wt.% NaCl. CNC (USDA) with 0.1 wt.% NaCl has already been explained in Figure 4, where adsorption seemed to be the most dominating mechanism at play. CNC (USDA) in 0.3 wt.% NaCl showed a similar trend in the transport behavior as CNC (AITF) in 0.1 wt.% NaCl (Fig.4). No significant adsorption is occurring as the NF BT-curve is overlaying with the tracer BT-curve in the beginning. The pressure slightly increased during the injection of the second PV of nanofluid and the post flush with brine had an early breakthrough. This suggests that log-jamming or blocking of pore throats inside the pack occurs. By blocking off pores, the pressure in the pack will increase as the permeability is reduced, and the fluid will have a smaller volume to traverse, which results in the early breakthrough. The overall permeability reduction with the higher salinity (0.3 wt.% NaCl) was 24 % (Table 4), and the pressure was almost three times higher compared to the injection with 0.1 wt.% NaCl.

The graph for the highest salinity is not included, as a filter-cake was created at the inlet of the sandpack. This resulted in 100% retained particles and 98 % permeability impairment (Table 4).

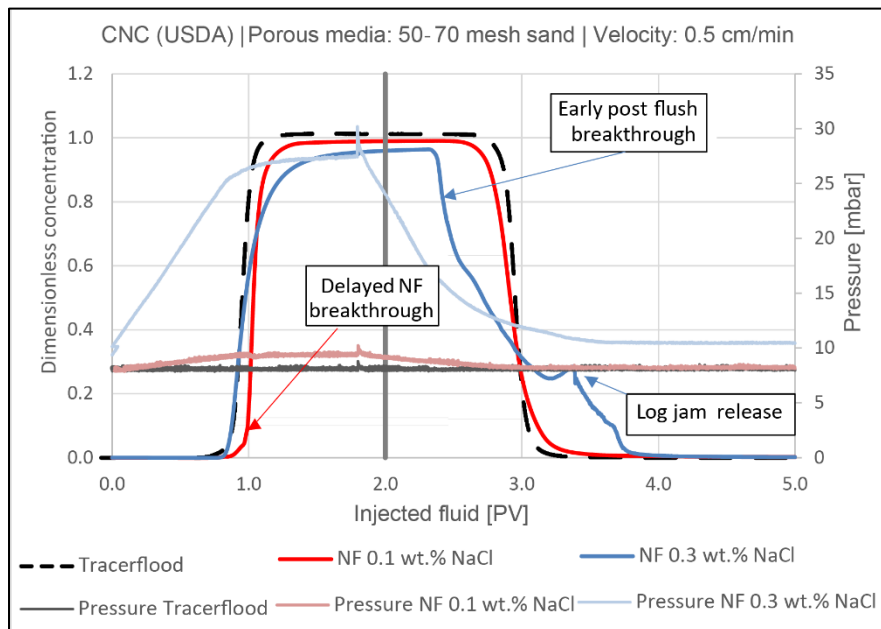


Figure 6. Breakthrough curve for flood with 0.5 wt.% CNC(USDA) in 0.1 wt.% NaCl (red line) and 0.3 wt.% NaCl (blue line). The tracer BT-curve is the black dotted line.

Table 4. Retained nanocellulose and permeability data from the flooding experiments.

Parameter changed	Retention [%]	Permeability [Darcy]		Permeability Reduction [%]
		Before	After	
1. Particle type				
CNC (USDA)	6.2	34	32	5.5
CNC (AITF)	6.6	36	31	13.3
2. Velocity				
0.1 ml/min	24.0	36	4	90.3
1.0 ml/min	6.6	36	31	13.3
8 ml/min	8.2	39	36	7.8
3. Grain size				
140-270 mesh	8.4	2.4	1.87	21.8
50-70 mesh	6.2	34	32	5.5
16-30 mesh	2.3	296	286	3.3
4. Salinity				
0.1 wt.% NaCl	6.2	34	32	5.5
0.3 wt.% NaCl	9.9	33	25	23.7
1.0 wt.% NaCl	100	34	0.9	97.5

Visualizing nanocellulose retention

To further elucidate that higher salinity results in higher retention and permeability impairment, visualization of the nanocellulose retention was performed using extensive heating of the post-flood sandpicks (Fig.7). For the flood with CNC (USDA) in 0.1 wt.% NaCl, it appears that the whole sandpick has darkened slightly. This suggests that nanocellulose filled adsorption sites in the pack resulting in a small retention. For the flood with high salt concentration, there is a notable darkening in the front while the outlet seemed to be unaffected. This indicates that the retention favored the front of the pack, which is consistent with a log-jamming phenomena leading to straining and filter cake formation. Both findings are consistent with the results from the BT-curves.

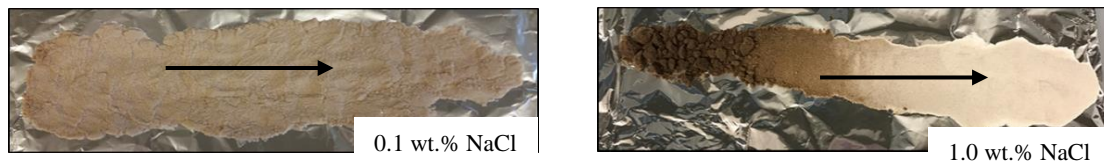


Figure 7. Burning photos of retention floods with CNC (USDA). The picture to the left is with 0.1 wt.% NaCl, while the picture to the right is with 1.0 wt.% NaCl. The arrow indicates the direction of flow.

CONCLUSION

- The two tested nanocellulose types were different in size. Particle size contributed to different transport behavior when flooded with 0.1 wt% NaCl.

- Salinity had the largest effect on retention, since it changed the aggregated particle size in the bulk solution.
- Smaller particles seemed to be dominated by adsorption on sand grains, whereas larger particles were retained in the sandpack by blocking and log-jamming.
- Retention and permeability reduction increases as the velocity decreases, the same trend is seen by decreasing the grain size.

ACKNOWLEDGEMENTS

The authors would like to thank the Research Council of Norway for their financial support through the grant 244615/E30 in the Petromaks2 programme. Also a big thank you to the Natural Sciences and Engineering Research Council of Canada for their financial support and for the use of the Canada Excellence Research Chairs laboratory at University of Calgary. This work was partly supported by the Research Council of Norway through its Centres of Excellence funding scheme, project number 262644. We also thank Alberta Innovates – Technology Futures for donating nanocrystal.

REFERENCES

- 1 Kamal, M. S., Sultan, A. S., Al-Mubaiyedh, U. A. & Hussein, I. A. Review on Polymer Flooding: Rheology, Adsorption, Stability, and Field Applications of Various Polymer Systems. *Polymer Reviews* **55**, 491-530, doi:10.1080/15583724.2014.982821 (2015).
- 2 Sun, X., Zhang, Y., Chen, G. & Gai, Z. Application of Nanoparticles in Enhanced Oil Recovery: A Critical Review of Recent Progress. *Energies* **10**, 345 (2017).
- 3 Klemm, D. *et al.* Nanocelluloses: a new family of nature - based materials. *Angewandte Chemie International Edition* **50**, 5438-5466 (2011).
- 4 Molnes, S. N., Torrijos, I. P., Strand, S., Paso, K. G. & Syverud, K. Sandstone injectivity and salt stability of cellulose nanocrystals (CNC) dispersions— Premises for use of CNC in enhanced oil recovery. *Industrial Crops and Products* (2016).
- 5 Ju, B. & Fan, T. Experimental study and mathematical model of nanoparticle transport in porous media. *Powder Technology* **192**, 195-202, doi:<http://dx.doi.org/10.1016/j.powtec.2008.12.017> (2009).
- 6 Dong, X. M., Revol, J.-F. & Gray, D. G. Effect of microcrystallite preparation conditions on the formation of colloid crystals of cellulose. *Cellulose* **5**, 19-32 (1998).
- 7 Heggset, E. B., Chinga-Carrasco, G. & Syverud, K. Temperature stability of nanocellulose dispersions. *Carbohydrate Polymers* **157**, 114-121 (2017).